Journal of Catalysis 428 (2023) 115143

Contents lists available at ScienceDirect

Journal of Catalysis

journal homepage: www.elsevier.com/locate/jcat

Highly cross-linked bifunctional magnesium porphyrin-imidazolium bromide polymer: Unveiling the key role of co-catalysts proximity for CO_2 conversion into cyclic carbonates

Laura Valentino [a], Vincenzo Campisciano [a], Chloé Célis [b], Vincent Lemaur [c], Roberto Lazzaroni [c], Michelangelo Gruttadauria [a,*], Carmela Aprile [b,*], Francesco Giacalone [a,*]

[a] Department of Biological, Chemical and Pharmaceutical Sciences and Technologies and INSTM UdR Palermo, University of Palermo, Viale delle Scienze, Ed. 17 90128, Palermo, Italy
[b] Laboratory of Applied Material Chemistry (CMA), Department of Chemistry, University of Namur, 61 rue de Bruxelles 5000, Namur, Belgium
[c] Laboratory for Chemistry of Novel Materials, Materials Research Institute, University of Mons – UMONS, Place du Parc 20, 7000 Mons, Belgium

ARTICLE INFO

Keywords:
Bifunctional Heterogeneous catalyst
Mg-porphyrin
Carbon dioxide fixation
Cyclic carbonates
Carbon nanotubes

ABSTRACT

Highly cross-linked materials containing an imidazolium salt and magnesium porphyrin, either in the absence (**TSP-Mg-imi**) or in the presence (**7a** and **7b**) of multi-walled carbon nanotubes (MWCNTs), were synthesized and used as heterogeneous bifunctional catalysts for the conversion of CO_2 into cyclic carbonates. The metalloporphyrin moiety acts both as a "covalent swelling agent", generating hybrids with high surface area, and as a Lewis acid co-catalytic species. **TSP-Mg-imi** produced excellent conversion and TON_{Mg} values, under solvent-free conditions, even at room temperature and with low catalytic loading (0.003 mol%). In terms of conversion and TON_{Mg}, **TSP-Mg-imi** exhibited better catalytic performance compared to a reference homogeneous system, demonstrating that the proximity between the metal centers and the nucleophilic site results in a synergistic effect during the catalytic cycle. The results of the computational study confirmed both the cooperative function and the significance of incorporating a co-catalytic species into the system.

1. Introduction

The transformation of carbon dioxide into valuable chemicals is an issue of growing interest because of its potential to convert industrial waste into a cheap, non-toxic, environmentally safe and sustainable carbon resource [1–6]. Carbon dioxide is essential in the production of a broad range of widely used chemical compounds including organic carbonates, urea derivatives, carboxylic acids, alcohols, and alkylamines [7–9]. Due to the highly oxidized state of the carbon atom in CO_2, its molecular reactivity is inherently low. To address this problem, highly energetic substances, such as small cyclic ethers, are used along with a catalyst that can reduce the activation energy required for the desired reaction. A convenient route to exploiting CO_2 is its fixation into epoxides for the production of cyclic carbonates,[10,11] which have found wide applications as polar aprotic solvents, electrolytes in lithium-ion batteries, fuel cells and intermediates in pharmaceutical chemistry [12,13]. This process is one of the most effective and promising synthetic routes in Green Chemistry, displaying an atom economy of 100 %. In addition, CO_2 can also replace toxic and flammable species such as phosgene, which is used industrially in the transesterification of polyols to obtain cyclic carbonates [14]. The transformation of epoxides into cyclic carbonates usually requires a nucleophile able to promote the epoxide ring opening. Moreover, the presence of a Lewis acid catalyst in the system can contribute to the activation of the epoxide for ring-opening and stabilization of the corresponding alkoxide. The two species can either be present in separate systems, known as binary catalysts, or can be incorporated into the structure of a bifunctional catalyst. Several catalytic systems, both homogeneous and heterogeneous, have been proposed for the conversion of CO_2 into cyclic carbonates by reaction with epoxides. Many organocatalysts and metallic complexes have been developed as homogeneous catalysts [15–25]. Organocatalysts are considered to be eco-friendly, cheap and accessible compounds, non-toxic in nature given the absence of metals in their structures, but their activity in CO_2 cycloaddition often needs to be enhanced by the co-participation of metal complexes. The Lewis acidity of a metal ion can promote the coordination and activation of the

* Corresponding authors.
E-mail addresses: michelangelo.gruttadauria@unipa.it (M. Gruttadauria), carmela.aprile@unamur.be (C. Aprile), francesco.giacalone@unipa.it (F. Giacalone).

https://doi.org/10.1016/j.jcat.2023.115143
Received 4 April 2023; Received in revised form 12 September 2023; Accepted 23 September 2023
Available online 26 September 2023

epoxide.

Even though homogeneous catalysts have high activity and catalytic efficiency, their recovery/recycling is quite complicated, making the purification of cyclic carbonates obtained highly tedious and energy intensive. To avoid these drawbacks and meet the needs of sustainable development and environmental protection, there is a paramount interest in the synthesis and use of recyclable catalytic systems. Heterogeneous catalysis is a beneficial process due to the green aspects it brings to catalysis. The easy separation, recovery and possible reusability of such catalysts make them a sustainable and green alternative to their homogeneous counterparts. Widely used in recent years are metal–organic frameworks (MOFs), porous organic polymers (POPs), silica-supported catalysts, and covalent organic frameworks (COFs) [26–30]. However, in most of these systems the nucleophilic species is used as a co-catalyst under homogeneous conditions, often in large quantities and not recovered. An effective solution to address these issues is to integrate both catalytic species within the same material, providing an alternative approach. Heterogeneous bifunctional catalysts [31–42] are interesting owing to their possible synergistic features. Among the metal complexes used as co-catalyst in the cycloaddition of CO_2 with epoxides, metalloporphyrins have raised considerable interest [43–45]. The geometry of complexation with the porphyrin is square planar, which allows incorporating various metal ions as Ni, Al, Zn, Co and Mg in the core of the porphyrin ring. Currently, only a few publications report the use of magnesium porphyrin for the design and preparation of both heterogeneous and homogeneous bifunctional catalysts [30,34,46–49].

In our previous work, we have shown that the cooperation/synergy between electrophilic and nucleophilic sites provides excellent catalytic activity for the conversion of cyclic carbonates from the reactions between CO_2 and epoxides [50,51]. Compared to materials with only a nucleophilic component,[52–57] these bifunctional materials display catalytic activity even under mild reaction conditions. In this study, we investigate the effect of Mg as Lewis acid center, focusing on the role played by the proximity between the two (co)catalysts on the overall catalytic performances. For that purpose, we use a joint experimental/computational approach to study the possible cooperation between Mg-porphyrin and bromide ions as counterion of imidazolium moieties when covalently linked. Ionic liquids (ILs), such as imidazolium salts, in which CO_2 shows a high solubility,[58–61] have been widely used and studied as catalysts for this type of reaction. The imidazolium counterions play a crucial role in the reaction mechanism by promoting the epoxide ring opening followed by the CO_2 insertion [62,63].

In terms of heterogeneous catalysis, carbon nanoforms are a family of carbon allotropes that are recently attracting a growing interest as supports due to their high surface area, high chemical inertness under many conditions, thermal stability and mechanical strength [64,65]. In particular, multi-walled carbon nanotubes (MWCNTs) have recently been used as catalytic support acting as useful templating agents during the radical polymerization of vinyl-imidazolium salts [50,66,67]. The resulting materials display a polymer network that covers the nanotubes along their entire length. This offers the advantage of obtaining a catalyst with more accessible sites, along with excellent robustness. Herein, highly-cross-linked materials containing imidazolium salt and magnesium porphyrin were thus designed. These materials were prepared by using a one-pot procedure either in the presence or in the absence of MWCNTs. Once characterized, their catalytic performance was evaluated in terms of recyclability, versatility, turnover number, turnover frequency and productivity values. Those catalysts showed good conversion and selectivity towards cyclic carbonates in a batch reactor configuration which allows working on a large scale and at high CO_2 pressures.

2. Materials and methods

Chemicals and solvents were purchased from commercial suppliers to be used without further purification. The syntheses of 1,4-butanediyl-3,3′-bis-1-vinylimidazolium dibromide (**5**) and magnesium tetrastyrylporphyrin (**TSP-Mg**) are reported in the Supporting Information section. Thermogravimetric analysis (TGA) was performed in a Mettler Toledo TGA STAR system with a heating rate of 10 °C/min, either under oxygen flow from 100 to 1000 °C or under nitrogen flow from 25 to 900 °C. Transmission electron microscopy (TEM) images were recorded using a Philips Tecnai 10 microscope operating at 80–100 kV. Nitrogen adsorption–desorption analyses were carried out at 77 K in a Micromeritics ASAP 2420 volumetric adsorption analyzer. Before the analysis the sample was pre-treated at 150 °C for 8 h under reduced pressure (0.1 mbar). The Brunauer-Emmett-Teller (BET) method was applied in the 0.05——0.30p/p_0 range to calculate the specific surface area. X-ray photoelectron spectroscopy (XPS) analyses were carried out in a ThermoFisher ESCALAB 250Xi instrument equipped with a monochromatic Al Kα X-ray source (1486.6 eV) and a hemispherical deflector analyzer (SDA) working at constant pass energy (CAE) allowing to obtain a constant energy resolution on the whole spectrum. The experiments were performed using a 200 μm diameter X-ray spot. The charge neutralization of the sample was achieved with a flood gun using low energy electrons and argon ions. The pressure in the analysis chamber was in the range of 10^{-8} Torr during data collection. Survey spectra were recorded with a 200 eV pass energy, whereas high-resolution individual spectra were collected with a 50 eV pass energy. Analyses of the peaks were carried out with the Thermo Avantage software, based on the non-linear squares fitting program using a weighted sum of Lorentzian and Gaussian component curves after background subtraction according to Shirley and Sherwood. Inductively coupled plasma optical emission spectroscopy (ICP-OES) was employed in an Optima 8000 Spectrometer. ^{1}H NMR spectra were recorded on a Bruker 400 MHz spectrometer. Solid state ^{13}C NMR spectra were recorded at room temperature on a JEOL ECZ-R spectrometer operating at 11.7 T using a 3.2 mm AUTOMAS probe and spinning frequencies of 10 kHz. FT-IR measurements were performed in absorbance mode using a Perkin Elmer two DEP. Chemical combustion analysis was performed on a Perkin-Elmer 2400 Serie 2 analyzer.

2.1. Synthetic procedures

2.1.1. Synthesis of highly cross-linked TSP-Mg-imi (6)

Under argon atmosphere, bis(vinyl)imidazolium salt **5** (327 mg, 0.809 mmol) and **TSP-Mg** (150 mg, 0.202 mmol) were transferred to a two-necked round bottom flask and dissolved in dry dimethylformamide (DMF) (5.6 mL). After the addition of azobis(isobutyronitrile) (AIBN) (5 wt%), Argon was bubbled into the mixture for 20 min, which was then refluxed and stirred at 120 °C overnight. The hybrid solid material was recovered by centrifugation and washed several times with DMF, chloroform and methanol. Before each centrifugation, the catalyst was sonicated for 10 min in the washing solvent. The last washing was done with diethyl ether. The green-colored catalyst was recovered and dried under vacuum at 60 °C (437 mg, 91 %).

2.1.2. Synthesis of MWCNT-TSP-Mg-imi 1:8 (7a) and MWCNT-TSP-Mg-imi 1:12 (7b)

In a two-neck round-bottom flask, bis(vinyl)imidazolium salt **5** (0.809 or 0.809 mmol), **TSP-Mg** (0.202 or 0.135 mmol), MWCNTs (100 or 50 mg) and dry DMF (10 or 5 mL) were transferred and sonicated for 20 min, under argon atmosphere. AIBN (5 wt%) was added to the reaction mixture, which was bubbled argon for 20 min. The mixture was then refluxed and stirred at 120 °C overnight. The solid was recovered by centrifugation and washed several times with DMF, chloroform and methanol. Before each centrifugation, the catalyst was sonicated for 10 min in the washing solvent. After drying under vacuum at 60 °C, **MWCNT-TSP-Mg-imi** was obtained as a green solid (555 mg, 96 % for **7a**;450 mg, 94 % for **7b**).

2.2. General procedure for the conversion of CO_2

The catalytic tests were carried out in a Cambridge Design Bullfrog batch reactor, with temperature control, pressure monitoring and mechanical stirring. In each test, a fine dispersion of the catalyst was added into the selected epoxide under solvent-free conditions. Once the reactor was closed, the mechanical stirring speed was set at 500 rpm. The mixture was purged with N_2 for 10 min and then pressurized with 25 bar of CO_2. After this, the temperature was increased with a ramp of 5 °C/min and kept to the required temperature during the reaction time. In selected case, a refill of CO_2 was carried out during the experiment to maintain the quantity of reagent required for the reaction. At the end of the reaction time, the reactor was cooled down to room temperature and slowly depressurized. The separation of the catalyst from the reaction mixture was easily performed by centrifugation (15 min, 4500 rpm). The supernatant solution was analyzed by ^{1}H NMR spectroscopy in $(CD_3)_2SO$ or in $CDCl_3$.

2.2.1. General recycling procedure for the conversion of CO_2

The stability of the materials was tested in the reaction between epichlorohydrin and CO_2. After each catalytic test, the catalyst was recovered by centrifugation and washed with toluene (4x40 mL), ethanol (4x40 mL) and diethyl ether. To get a good dispersion, before each centrifugation, the catalyst was previously sonicated in the washing solvent for 15 min. Then, the solid was dried under vacuum at 60 °C. Once dried, the catalyst was reused for the next cycle keeping the ratio between moles of catalyst and moles of epoxides constant. The conversion of epichlorohydrin into cyclic carbonate was estimated by ^{1}H NMR analysis.

2.2.2. Reaction conditions of Scheme 2

The catalytic experiments of Scheme 2 were performed in a Teflon vial, under solvent-free conditions. In each test, the same amount of epichlorohydrin (24 mL, 306 mmol) was added. The comparison of the catalytic activity of the six systems was studied considering the Mg loading (0.019 mmol) and consequently the mass amount used of **TSP-Mg-imi 6** (60 mg). Therefore, the electrophilic center component (**TSP-Mg**) inserted was 15 mg, while the nucleophilic component (**Homopolymer** and **Bis-imi 5**) was 45 mg. After closing the reactor, the mixture was stirred at 500 rpm. The system was then purged for 10 min with N_2 before the addition of 25 bar of CO_2. After this, the system was heated to 80 °C with a heating rate of 5 °C/min. The conversion of epichlorohydrin into cyclic carbonate was estimated by ^{1}H NMR analysis.

2.3. Quantum-chemical calculations

All the quantum-chemical calculations have been performed in the Density Functional Theory (DFT) formalism with the Gaussian16 package using the M062X functional and the 6-311G* basis set. In all cases, the dispersion interactions were corrected with the D3 version of Grimme's dispersion with Becke-Johnson damping [68]. The complexation energies are estimated as the energy difference between the product and isolated reactants taking into account the correction for the basis set superposition error [69].

To simulate the nucleophilic attack of Br^-, a bromide anion has been bound in four different ways on the two carbons of the epoxy ring. The geometry of those species has then been first optimized while keeping the C–Br^- bond fixed at 1.96 Å before performing a full optimization of the complexes. In route 1 (Fig. 9 and **Figure S17**), the results point to the opening of the epichlorohydrin upon addition of the bromide anion, but the resulting activated oxygen does not react spontaneously with CO_2; an additional activation energy barrier has to be crossed. Determining the height of this activation energy barrier is beyond the scope of this study. Instead, we put CO_2 in closer contact (distance of 1.42 Å) with epichlorohydrin and reoptimized the assembly.

3. Results and discussion

New hybrid materials **TSP-Mg-imi 6** and **7a** were designed and prepared (Scheme 1) to be applied as heterogeneous catalysts for the synthesis of cyclic carbonates from the addition of carbon dioxide to various epoxides. Initially, the synthesis of **TSP-Mg 2** was achieved through the complexation of TSP **1** with magnesium bromide ethyl etherate ($MgBr_2$•OEt_2), whereas bis(vinyl)imidazolium **5** was quantitatively obtained by reaction of 1-vinylimidazole **3** and 1,4-dibromobutane **4**. Afterward, **TSP-Mg-imi 6** and **7a** were easily prepared by the radical copolymerization of bis(vinyl)imidazolium **5** and **TSP-Mg** mediated by thermal decomposition of azobis(isobutyronitrile) (AIBN) in refluxing DMF. In the case of **7a**, the radical polymerization was performed in the presence of MWCNTs as a support and templating material. The objective behind this approach was to improve the final specific surface area of the polyimidazolium copolymer, thereby enhancing the availability of active sites. Previous studies have indicated that unsupported polyimidazolium cross-linked networks exhibit significantly low specific surface areas [70–72]. In addition, monomer **5** was also polymerized to give **Homopolymer 8**, in order to compare the catalytic activity of the two hybrids. Catalyst **7b** was prepared with a different **TSP-Mg/Bis-imi** ratio (1:12) as a consequence of the results obtained with **TSP-Mg-imi 6** and **7a** and will be discussed below.

To investigate the structures and morphologies of the obtained materials, several analytical and spectroscopic characterization techniques were used. The morphological properties of **TSP-Mg-imi** and **7a**, in terms of specific surface area (BET), were determined by N_2 adsorption/desorption measurements (Fig. 1). According to the IUPAC classification, both co-polymeric cross-linked networks exhibit a type II isotherm typical of macroporous adsorbent with H3 hysteresis loop [73]. The supported copolymer **7a** (Fig. 1**b**) has a very low specific surface area (36 m^2/g) compared to **TSP-Mg-imi,** which displays a much higher value (216 m^2/g).

This value is surprisingly high, compared to almost all poly(ionic liquid)s, including **Homopolymer 8** (Figure S1), which are mostly non-porous or have a low-specific surface area [70–72,74–76]. This difference could be ascribed to the presence of magnesium porphyrin, which probably plays a role of swelling agent. Indeed, the presence of the porphyrin structure allows obtaining a more flexible polymer network in which the catalytic active sites are more accessible. In the case of **7a**, the effect of swelling agent by porphyrin is not observed, resulting in a material with a low specific surface area. To better understand this discrepancy, additional studies were conducted on the morphology of the two materials.

The characterization *via* transmission electron microscopy (TEM) of **TSP-Mg-imi** confirms the above hypothesis (Fig. 2): **TSP-Mg-imi** is a self-condensed polymeric material with an open network constituted by non-ordered macroporosity (thus displaying potential highly accessible catalytic active sites) (Fig. 2**a-c**). In contrast, **7a** forms a physical mixture consisting of supported and not supported copolymer (Fig. 2**e-f**). In this case, a limited templating effect of the MWCNTs can be noticed in comparison with our previous findings [50,55,67,72]. Overall, those TEM micrographs reflect the difference between the two materials in terms of specific surface area.

Scanning electron microscopy with energy dispersive X-ray spectroscopy (SEM/EDX) has been used to investigate the chemical composition of **TSP-Mg-imi** and **7a** (Fig. 3 and Figure S2). In particular, the presence in the **TSP-Mg-imi** network of both active sites, magnesium and bromide, is verified with EDX-mapping and no significant separate domains are observed (Fig. 3**e and 3c**).

Solid-state ^{13}C NMR spectroscopy was carried out using the Cross-Polarization Magic Angle Spinning Total Suppression of spinning side bands technique (CP-MAS-TOSS ^{13}C NMR) (Fig. 4). The spectra for both materials confirmed the success of the polymerization as evidenced by the absence of signals around 110 ppm corresponding to the vinyl = CH_2 groups, which are now present as methylene signals in the range

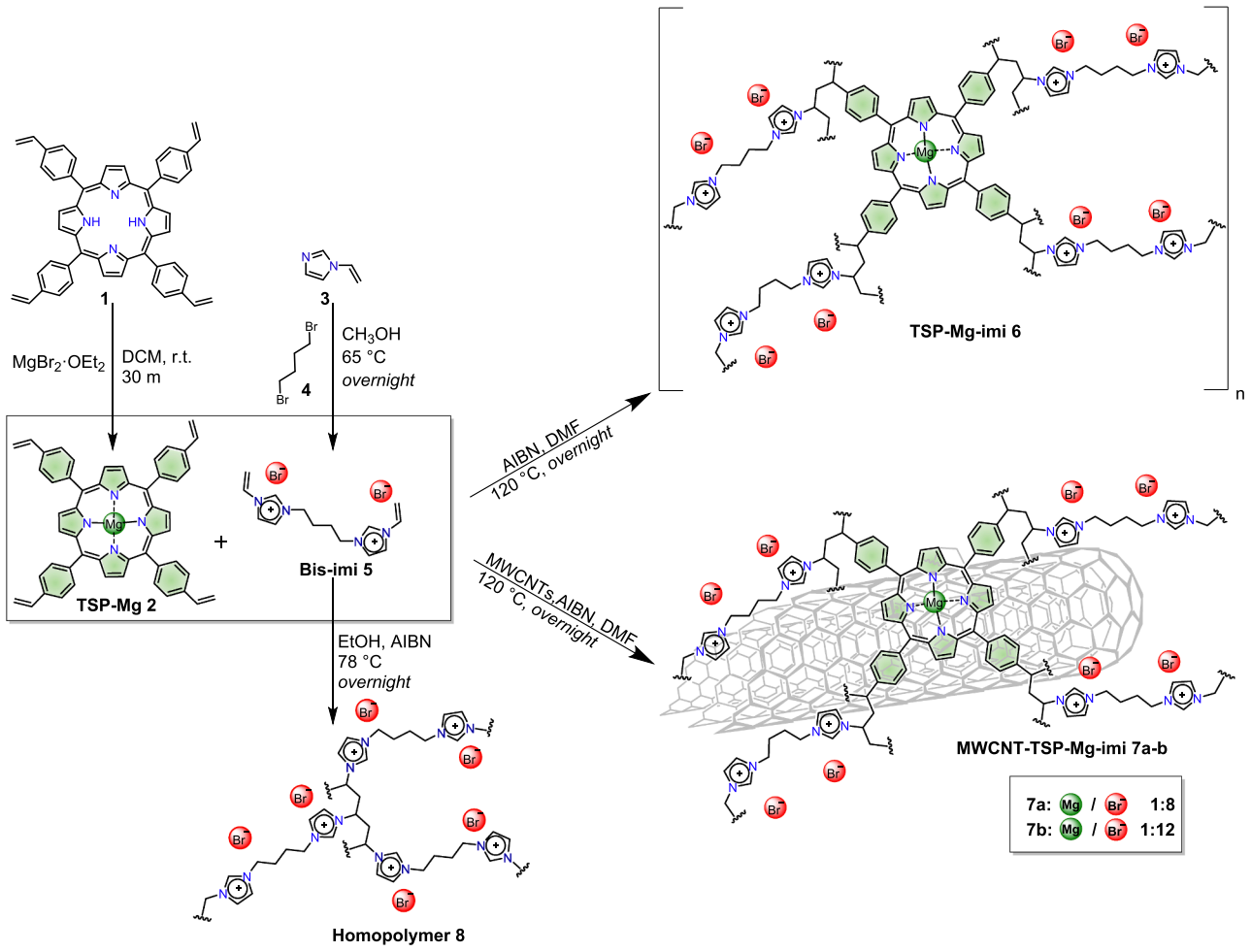

Scheme 1. Synthetic procedure for the preparation of **TSP-Mg-imi 6** and **7a-b**.

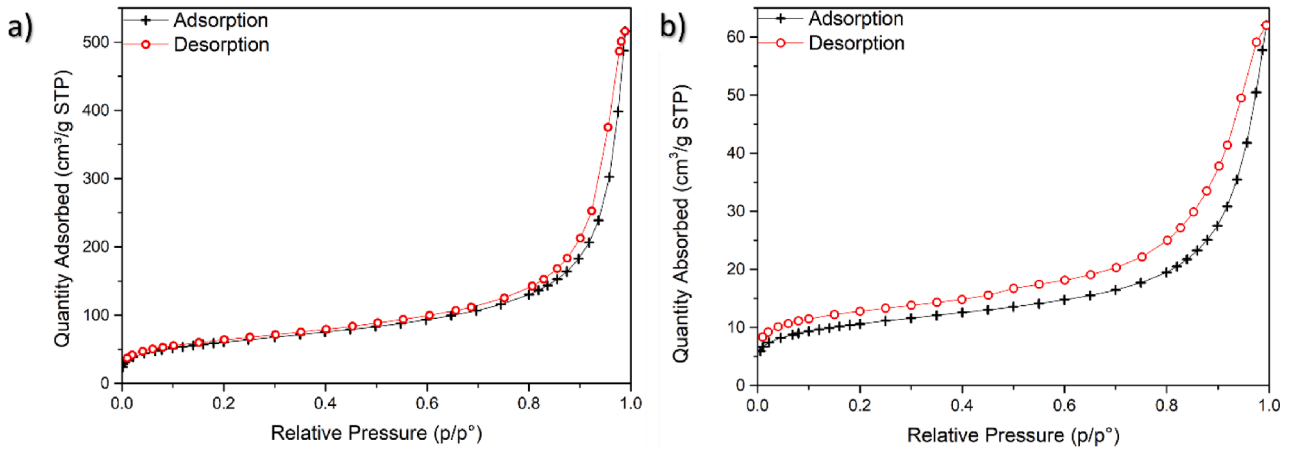

Fig. 1. Nitrogen adsorption–desorption isotherms of (a) **TSP-Mg-imi**, and (b) **7a**.

between 20 and 60 ppm. The aliphatic carbons that form the linker between the imidazolium rings also resonate in this region. In addition, at low field (110–150 ppm), the signals referring to the aromatic carbon atoms of the porphyrin and imidazolium moieties are present.

The thermal behavior of the new hybrid materials was investigated using thermogravimetric analysis - TGA (Fig. 5). Under nitrogen flow, **TSP-Mg-imi** and **7a** (yellow and green curves) show a good thermal stability, with decomposition of the organic backbone beginning around 250 °C. In addition, the TGA profile under air flow of **TSP-Mg-imi** (Figure S3) confirms the thermal robustness of the material, which is promising for its possible repeated use under heating conditions. TGA in air also allows estimating the Mg content (1.4 %, as MgO) from the residual weight percentage at 800 °C, corresponding to a Mg(II) loading of 0.35 mmol/g. On the contrary, the Mg content in **7a** cannot be estimated using this technique, as the fixed residue is made of both magnesium in the form of MgO and MWCNTs (Figure S3). The Mg content of **7a** (0.39

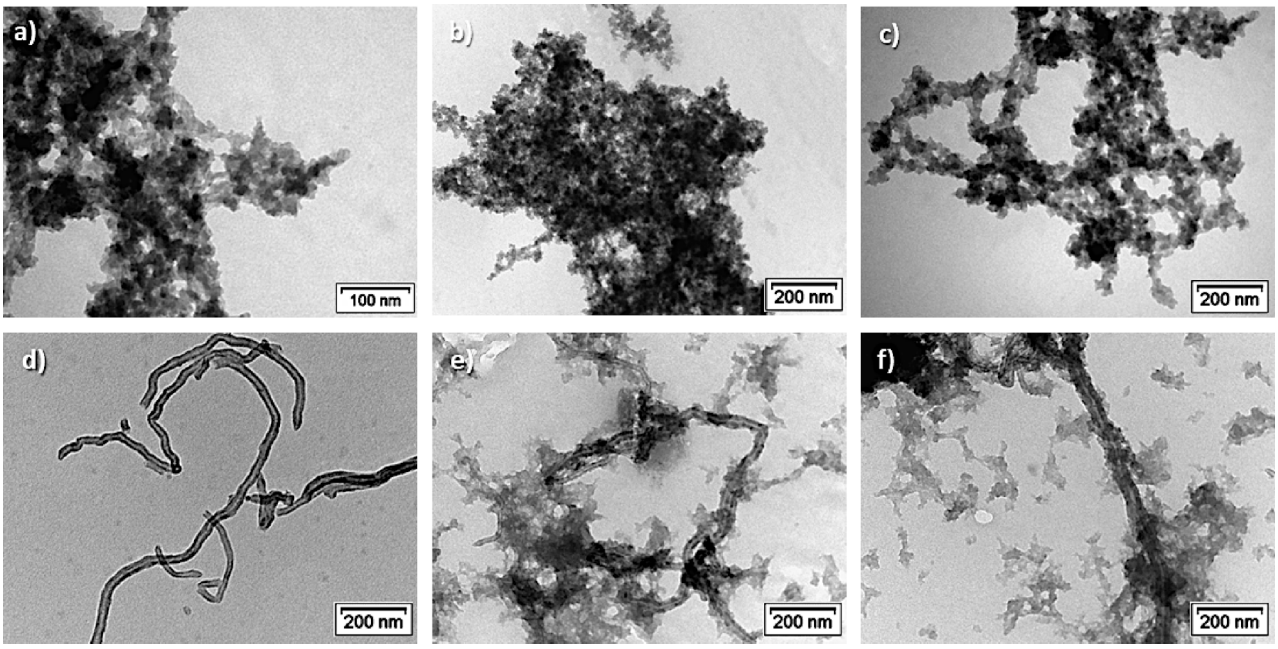

Fig. 2. TEM micrographs of **TSP-Mg-imi** (a-c), pristine-MWCNT (d) and **7a** (e-f).

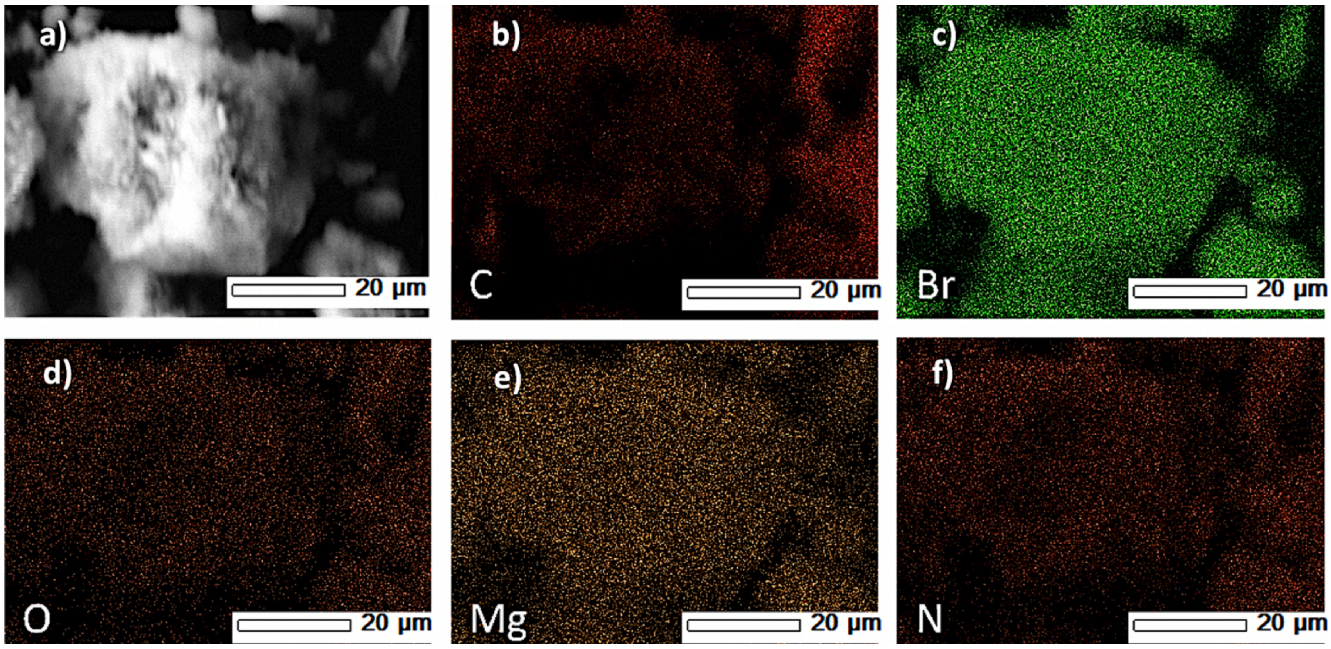

Fig. 3. (a) SEM image of **TSP-Mg-imi**, (b-f) EDX elemental-mapping images of **TSP-Mg-imi**.

mmol/g) was determined using inductively coupled plasma atomic emission spectroscopy (ICP-OES) analysis; the corresponding value for **TSP-Mg-imi** (0.33 mmol/g) is very similar to the one evaluated via TGA.

Furthermore, both materials **TSP-Mg-imi** and **7a** were subjected to XPS analysis to evaluate the presence of the active sites Mg/Br^- (Fig. 6 and Figure S4). The survey spectrum of **TSP-Mg-imi** (Fig. 6**a**) confirms the signatures of the metal at 1305 eV (Mg 1 s) and of the nucleophilic sites of the catalyst at 254, 180 and 67 eV, respectively (Br 3 s, Br 3p and Br 3d). In addition, the high-resolution N 1 s spectra display three peaks with distinct binding energies that can be attributed to the nitrogen of the imidazolium moieties at 401.3 eV and the nitrogen of the porphyrin at 400 and 398 eV (Fig. 6**b**). The splitting in two peaks for the metalloporphyrin is not surprising and has already been described in the literature; it is due to the partial demetallation of the **TSP-Mg** during its prolonged exposure to X-ray [77–79]. Hence, an approximate 1:4 ratio between the areas of the peaks of Mg–N (green and blue lines) and imidazolium–N (red line) was determined by XPS analysis (Fig. 6**b**). This value agrees with the Mg/Br^- stoichiometric ratio of 1:8. On the contrary, in **7a** this ratio is not respected; the atomic percentages of the two different nitrogen atoms are 39 % and 61 % for Mg–N and imidazolium–N, corresponding to 1/1.5 ratio (Figure S4).

The nitrogen content of **TSP-Mg-imi** was also estimated by combustion chemical analysis (Table S1). Through this value and considering the atomic percentage of N–Mg (green and blue lines) from the XPS analysis, it was possible to extrapolate a magnesium content of 0.34 mmol/g, in accordance with the previous reported techniques.

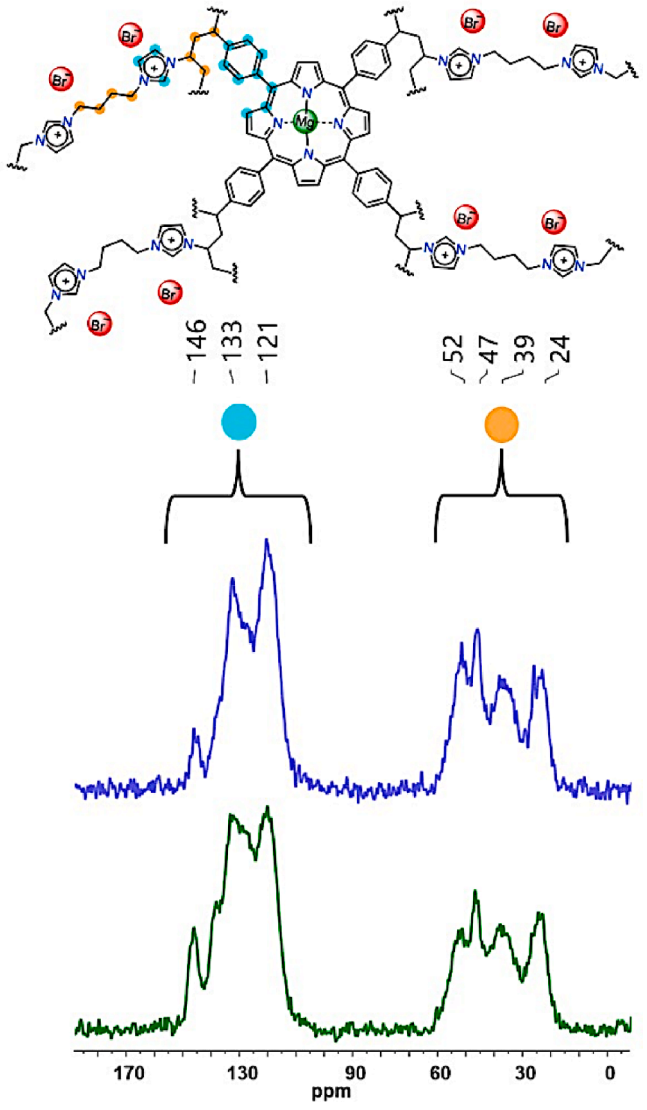

Fig. 4. ^{13}C CP-MAS-TOSS NMR of **TSP-Mg-imi** (blue line) and **7a** (green line).

In order to investigate the role of **TSP-Mg-imi** and **7a** as heterogeneous catalysts, both hybrids were studied in the synthesis of cyclic carbonates under solvent-free conditions. The catalytic performances were evaluated in terms of turnover number (TON_{Mg}, calculated as moles of epoxide converted/moles of Mg active sites), turnover frequency (TOF_{Mg} = TON_{Mg}/reaction time in hours), productivity (P, calculated as grams of cyclic carbonates obtained *per* grams of catalyst). and recyclability. All catalytic tests were performed in a batch-type reactor operating with large amounts of epoxide (200 mmol, cca 20–25 mL) leaving a headspace over the liquid surface of ~ 25 mL. Therefore, in our case, the use of high pressures not only allows significant volume reduction, since atmospheric CO_2 would require significantly more volume than the pressurized gas but, most importantly, allowed us to have enough CO_2 to convert the epoxide. In addition, the conditions adopted here are particularly relevant because they are similar to those normally used on an industrial scale, and thus only minor adjustments would be needed to move the preparations reported here to a larger scale.

The reaction between carbon dioxide and epichlorohydrin was selected for a preliminary investigation (Fig. 7). The recycling efficiency of the hybrid solids was evaluated over four catalytic runs at 60 °C. At the end of each catalytic cycle, the catalyst was recovered from the reaction mixture by centrifugation and washed with toluene, ethanol, and

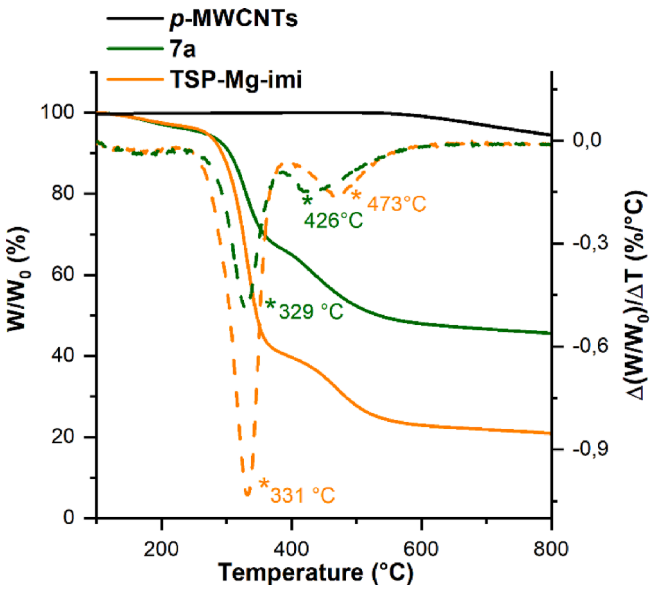

Fig. 5. TGA (sold lines) analysis under N_2 and DGT (dotted lines) flow of pristine MWCNTs (black line), **7a** (green line) and **TSP-Mg-imi** (yellow line).

diethyl ether without any additional activation treatment.

The results illustrated in Fig. 7, show that: (i) both the **TSP-Mg-imi** and **7a** catalysts can be reused in multiple catalytic cycles without any considerable decrease of the catalytic activity, and (ii) the TON_{Mg} performance of **TSP-Mg-imi** is significantly better than that of the supported hybrid solid. At this stage, it is not possible to discern whether the lower activity of **7a** is due to a possible negative influence of the nanotubes, or if it is a consequence of the lower specific surface area of the material or if it is caused by a non-optimal Mg/Br^- ratio, as highlighted by XPS analyses.

To address those questions, a second MWCNTs hybrid material, called **7b**, was prepared by changing the porphyrin/bis imidazolium salt ratio (Mg/Br^-) in the feed from 1:8 to 1:12, in order to obtain a catalyst with a Mg/Br^- ratio closer to 1:8, as in TSP-Mg-imi. The morphological analysis of **7b** (Fig. 8) reveals that the cross-linked polymer now covers the nanotubes, resulting also in an enhancement of the specific surface area to 174 m^2/g (Figure S5).

XPS analysis confirmed that the selected feed stoichiometry was appropriate since a 1:8 Mg/Br^- ratio has been achieved in the final material (Figure S6). Subsequently, the new catalyst **7b** was tested under the same reaction conditions and a clear enhancement compared with **7a** has been achieved (Fig. 7). This marked difference can be now explained by the homogeneity of the new hybrid, uniformly supported on the MWCNTs, the resulting increase in surface area and a more adequate Mg/Br^- ratio. The new hybrid material **7b** and the copolymer **TSP-Mg-imi** exhibit a quite similar catalytic activity. Nevertheless, considering the excellent performance of the unsupported copolymer, it was decided to focus the study on this hybrid material. Indeed, **TSP-Mg-imi** results more appealing from an economic and environmental point of view, since this bifunctional catalyst has been designed and prepared using only two components, without any waste. From a morphological point of view, its porous structure and the unexpected high surface area allow excellent dispersion of the active sites, as well as good diffusion of reactants during the reaction process. The catalytic performance of **TSP-Mg-imi** was then studied at different temperatures, again choosing epichlorohydrin as benchmark substrate.

As shown in Table 1, the conversion values of epichlorohydrin range from 24 % at room temperature to 95 % when the temperature is increased up to 100 °C. These values show the good catalytic activity of **TSP-Mg-imi** even at room temperature. Indeed, the conversion increases from 24 % at room temperature (24 h) to 32 % at 60 °C (3 h) with 120

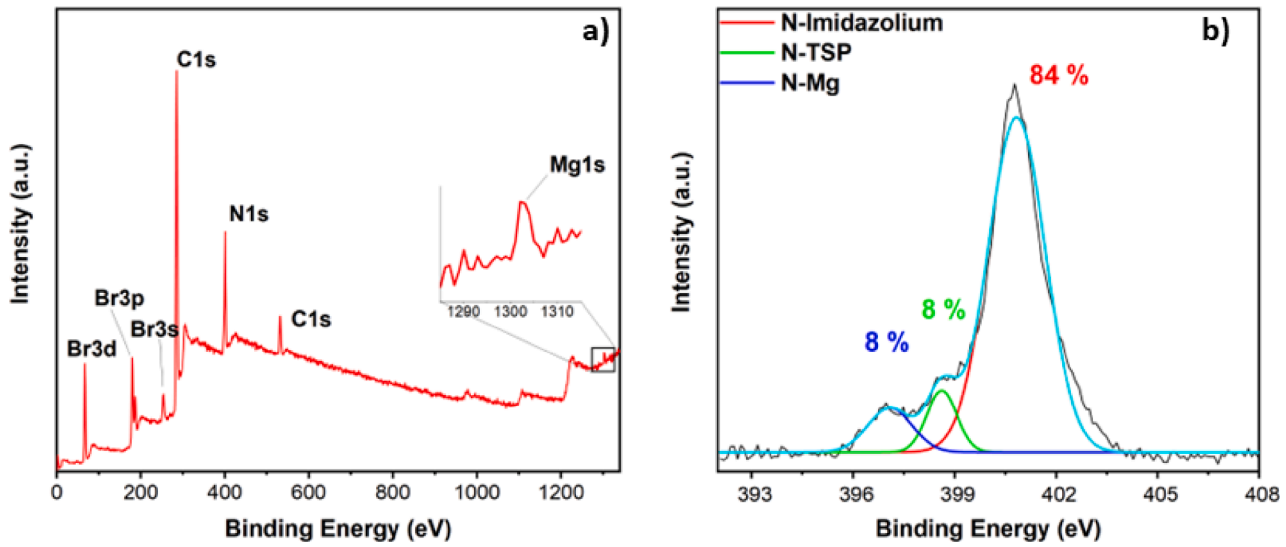

Fig. 6. XPS Survey spectrum of **TSP-Mg-imi** (a) and high-resolution N 1 s region (b).

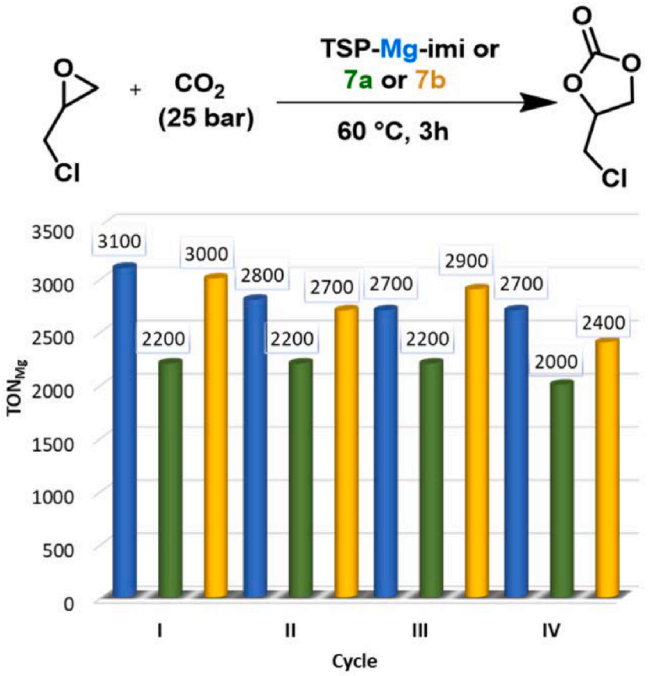

Fig. 7. Comparison of the TON_{Mg} values for **TSP-Mg-imi** (blue), **7a** (green) and **7b** (yellow) over four catalytic cycles in the reaction of epichlorohydrin with CO_2. Reaction conditions: epichlorohydrin (382 mmol), catalyst (**TSP-Mg-imi** 0.039 mmol Mg or **7a** 0.045 mmol Mg or **7b** 0.022 mmol Mg), 25 bar CO_2, 60 °C, 3 h, 500 rpm.

mg of catalyst corresponding to 0.010 mol% (entries 1 and 2). The effect of the temperature on the conversion is clear when the title reaction has been carried out at 80 °C with half the amount of catalyst (0.006 mol%) yielding an 80 % conversion (entry 3) and almost total conversion (>95 %) when the temperature was further increased up to 100 °C (entry 4), achieving a TON of 15300. When the reaction was conducted in one hour, epichlorohydrin was converted into the cyclic carbonate with a conversion of 70 %. (entry 5). Finally, considering the excellent results obtained at 100 °C, two additional tests were conducted aimed to further reduce the amount of catalyst to 30 mg, 0.003 mol% (entry 6). Although the catalytic loading has been decreased, a very good conversion of 66 % with a TON_{Mg} value of 20,400 has been obtained, when the system was maintained with a constant pressure of CO_2 (10 bar). A further improvement in terms of conversion and TON_{Mg} has been achieved by increasing and maintaining the working pressure of CO_2 at 25 bar, allowing to reach 80 % conversion into the corresponding cyclic carbonate, which resulted in a TON_{Mg} of 24,700 (entry 7).

A more detailed study of the catalytic activity of **TSP-Mg-imi** was carried out by performing additional tests. Scheme 2 shows the synthesis of epichlorohydrin carbonate at 80 °C for 3 h using different catalytic systems. **Homopolymer 8**, synthesized via polymerization of **Bis-imi 5**, and **Bis-imi 5** itself were used as the source of Br^- as heterogeneous and homogeneous systems, respectively (Scheme 2). Three different systems were tested using **TSP-Mg** as Lewis acid: (a) **TSP-Mg** alone; (b) a combination of **TSP-Mg** and **Homopolymer**; (c) a combination of **TSP-Mg** and **Bis-imi**. For each test performed, the amount of catalyst was based on the Mg loading of the catalyst in the reference reaction, **TSP-Mg-imi** (19 μmol). The **Homopolymer** as well as the [**Homopolymer** + **TSP-Mg**] system, under the title conditions, display no catalytic activity (reactions 1–2). This result can be attributed to the low value (<1 m^2/g) of the specific surface area of the homopolymer (Figure S1). Also, **TSP-Mg** alone shows no conversion of epoxide (reaction 3). Under homogeneous conditions **Bis-imi** alone gave a low conversion (12 %), whereas when the co-catalyst **TSP-Mg** is added, the conversion is boosted, reaching 60 % (reactions 4–5). These results show the importance of the co-catalyst in the system. Finally, the catalytic test with **TSP-Mg-imi** was repeated (Table 1, entry 4), thus confirming the good reproducibility of the hybrid material (reaction 6). These results are summarized in Scheme 2.

Comparing the homogeneous [**Bis-imi** + **TSP-Mg**] system with the heterogeneous catalyst, TON_{Mg} values are quite similar (reactions 5–6) but with the clear advantage of easy recovery and reuse of the heterogeneous catalyst through a simple filtration and, considering the mass transfer limitations for heterogeneous catalysis. It can be hypothesized that the improved catalytic performance shown by the bifunctional polymeric catalyst stems from the direct linking between the two active parts, namely the porphyrin core and the bis(vinyl)imidazolium salt. This ensures the spatial proximity between the metal centers and the bromide ions, which can cooperate more efficiently, resulting in a synergistic effect during the catalytic cycle for the formation of the cyclic carbonates.

To support this hypothesis a catalytic test, in which the proper amount of **Bis-imi** was added to **7a,** was performed. In this way, the optimal Mg/Br^- ratio, such as that found in **7b**, was reached. This addition of the homogeneous bromide source, namely **Bis-imi**, showed

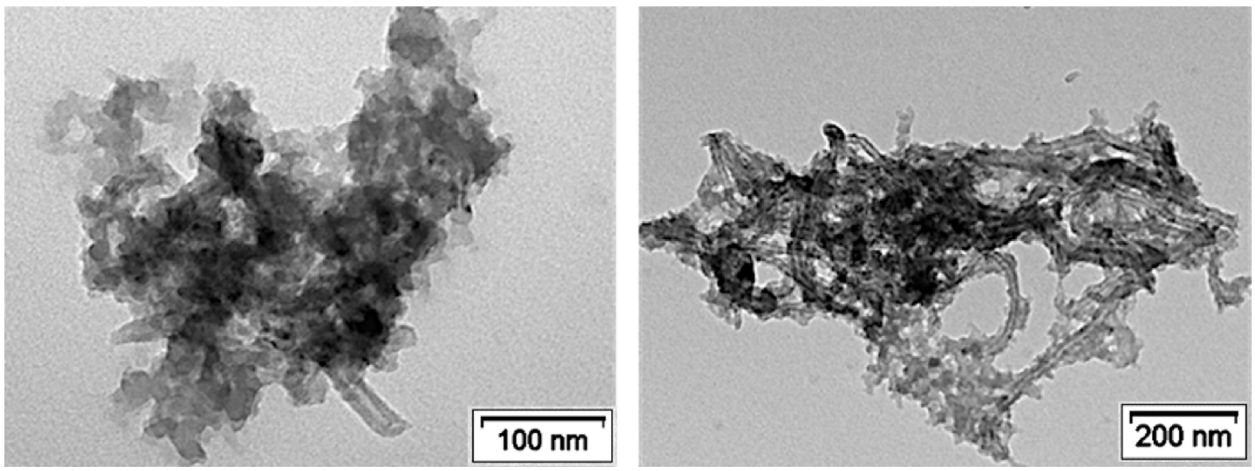

Fig. 8. TEM micrographs of hybrid **7b**.

Table 1
Epichlorohydrin carbonate synthesis catalyzed by **TSP-Mg-imi**[a].

Entry	Substrate	t (h)	T (C°)	Conversion (%)[b]	TON_{Mg}[c]	TOF_{Mg} (h^{-1})[c]	Productivity[d]
1[f,e]	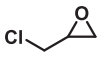 306 or 382 mmol	24	30	24	2400	100	100
2[e,f]		3	60	32	3100	1000	100
3		3	80	65	10,500	3500	400
4		3	100	95	15,300	5100	700
5		1	100	70	11,300	11,300	500
6[g,h]		3	100	66	20,400	6800	900
7[g,i]		3	100	80	24,700	8200	1100

[a] Reaction conditions: CO_2 (25 bar), epichlorohydrin (306 mmol), catalyst 60 mg (0.019 mmol Mg), 500 rpm.
[b] Determined by ^1H NMR.
[c] TON_{Mg} and TOF_{Mg} values calculated based on the Mg content obtained from ICP analysis.
[d] productivity (P, calculated as grams of cyclic carbonates obtained *per* grams of catalyst).
[e] Epichlorohydrin 382 mmol.
[f] Catalyst 120 mg (0.039 mmol Mg).
[g] Catalyst 30 mg (0.009 mmol Mg).
[h] CO_2 constant pressure 10 bar.
[i] CO_2 constant pressure 25 bar.

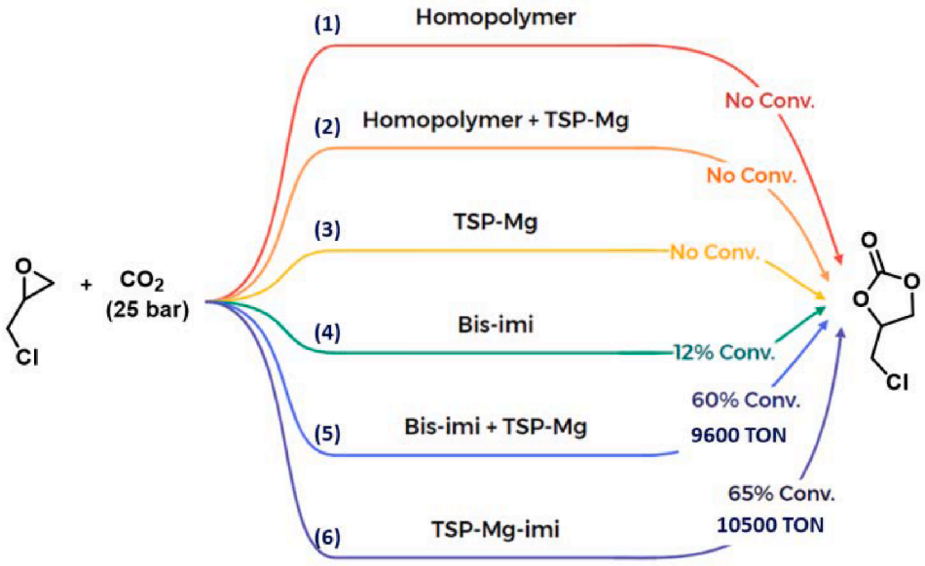

Scheme 2. Comparison of the catalytic activity between the heterogeneous system **TSP-Mg-imi**, **Homopolymer** and **Homopolymer** + **TSP-Mg** and the homogenous systems **Bis-imi**, **Bis-imi** + **TSP-Mg** and **TSP-Mg** in the reaction of epichlorohydrin with CO_2. Reaction conditions of tests 1–6 are reported in Section 2.2.2.

no improvement concerning the previously obtained TON_{Mg} value (Fig. 7), further indicating that covalently linked co-catalytic moieties behave more efficiently than the homogeneous counterpart.

To verify this hypothesis, the energetics of two different catalytic routes have been estimated at the quantum-chemical level (M062X/6-311G*/GD3BJ), see details in the Materials and Methods section. On one hand (route 1, see Fig. 9 and **Figure S17**), tetraphenyl porphyrin, TPP-Mg, is first activating epichlorohydrin; as a result, the oxygen atom is

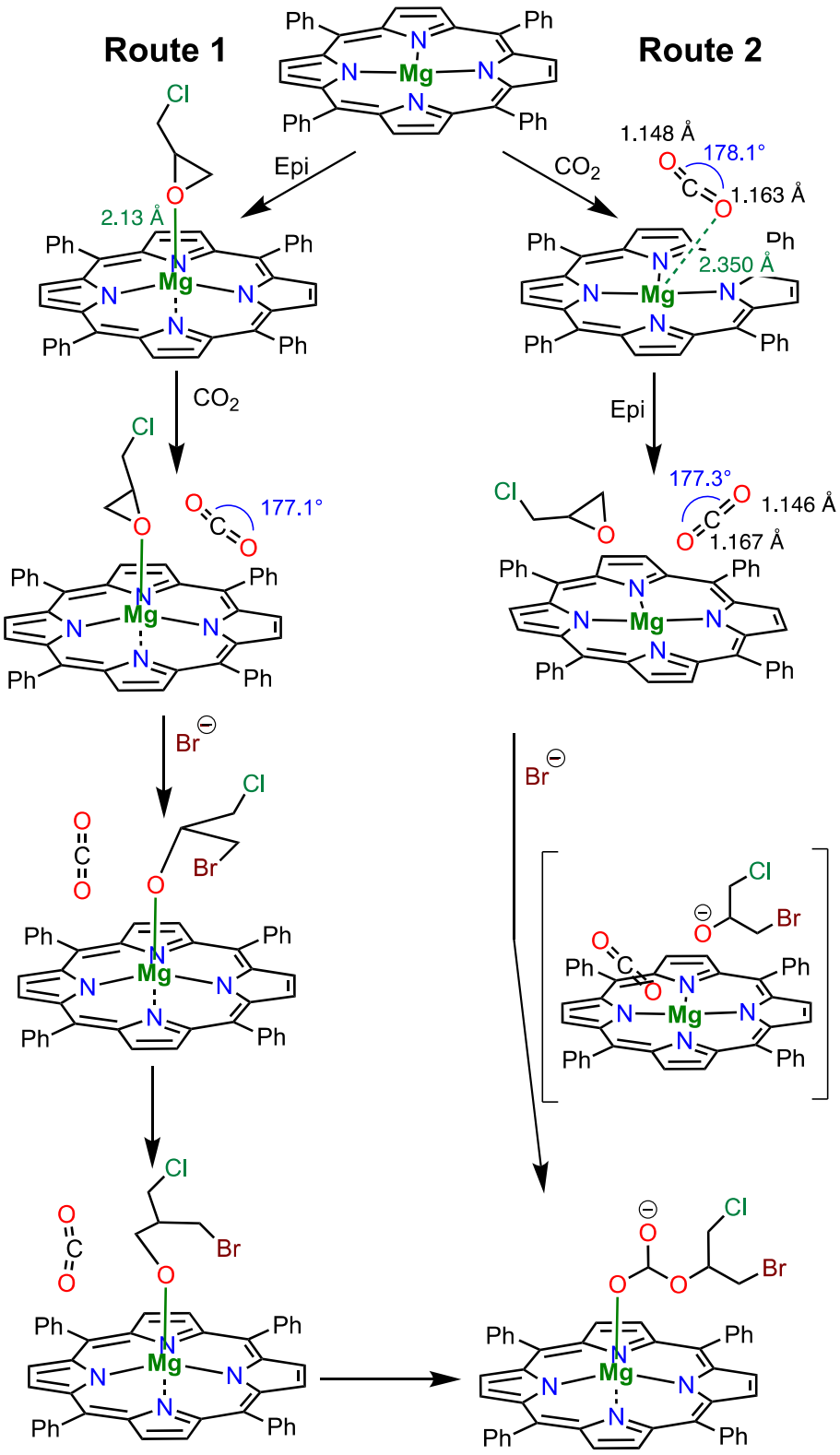

Fig. 9. Representation of the two catalytic routes investigated at the quantum-chemical level (M062X/6-311G*/GD3BJ). The structure between brackets is a representation of the intermediate formed upon the bromide anion nucleophilic attack but does not correspond to a stable energy minimum. Epi stands for epichlorohydrin.

clearly interacting with the metal center, the Mg-O distance being about 2.13 Å. On the other hand (route 2), it is CO_2 that first interacts with TPP-Mg. In that case, the CO_2 molecule is found to bend slightly (O–C–O angle of 178.1°) and gets nonsymmetric upon interaction with TPP-Mg: the C–O bond involving the activated oxygen becomes longer (1.163 Å *versus* 1.148 Å). In that complex, the closest Mg–O contact is 2.350 Å. Comparing the first step in the two routes, our calculations clearly point to more stabilizing interactions of TPP-Mg with epichlorohydrin, the complexation energies being 23.1 kcal/mol and 8.9 kcal/mol for epichlorohydrin and CO_2, respectively.

Once the second reactant, i.e., either CO_2 (route 1) or epichlorohydrin (route 2), is added to the systems, the more stable complex (-7.9 kcal/mol) is still when epichlorohydrin is interacting primarily with TPP-Mg. The CO_2 molecule is getting even more nonsymmetric in route 2 in the presence of epichlorohydrin (O–C–O angle of 177.3°, C–O bonds of 1.167 Å and 1.146 Å), whereas it remains symmetric but bends in route 1 (O–C–O angle of 177.1°). The more stable complex (epichlorohydrin-TPP-Mg) points up the importance of synthesizing a material in which the two active catalytic sites are covalently linked. Indeed, the close spatial proximity between the porphyrin ring and the imidazole group, as well as the presence of bromide ions, result in a material with significantly improved catalytic efficiency.

The computational results also show that, once the bromide ion is reacting with epichlorohydrin (see details in the Materials and Methods section), the three-membered ring opens and the resulting activated oxygen spontaneously attacks the carbon atom of CO_2 when the latter is interacting with TPP-Mg (route 2). In route 1, the opened epichlorohydrin also reacts with CO_2 but this requires crossing an energy barrier. Even in route 1 for which epichlorohydrin is initially in interaction with the Mg atom, the reaction with CO_2 leads to a rearrangement of the epichlorohydrin-CO_2 complex in such a way that the reaction ends up with the same product as in route 2. We thus believe that the complex shown at the bottom right of Fig. 9 reliably represents the species appearing upon reaction between epichlorohydrin and CO_2 in the presence of TPP-Mg and bromide ions.

Finally, the overall versatility of **TSP-Mg-imi** was explored using other epoxides such as 1,4-butanediol diglycidyl ether, propylene oxide or the more challenging cyclohexene oxide, styrene oxide and oxetane (Table 2).

In all the catalytic tests, good conversions to the corresponding cyclic carbonates were achieved, as well as good TON and productivities. Due to the high steric hindrance of the reactant, reaction with cyclohexene oxide required a longer reaction time (24 h) at 150 °C (entry 1). **TSP-Mg-imi** showed full selectivity toward the corresponding cyclic carbonate with a conversion of 75 %. In addition, a *cis/trans*-cyclohexene carbonate ratio of 94:6 was detected by ^{1}H NMR. Styrene oxide was converted at 56 % into the corresponding carbonate after 3 h (entry 2). The reaction with 1,4-butanediol diglycidyl ether was run at 125 °C affording quantitative conversion into the corresponding cyclic carbonate in 20 h (entry 3). The reactivity of propylene oxide was explored at 100 °C, with a reaction time of 3 h and applying a catalytic loading of 0.019 mmol Mg. Overall, a good conversion of 32 % was obtained with a TON_{Mg} value of 6000 (entry 4). Using oxetane as a substrate, 70 % of conversion was achieved, with very high selectivity toward the polycyclic carbonate product (entry 5). This value can be attributed to the combination of the high operating temperature and the presence of Mg, which plays a coordinating effect during the catalytic process [80].

Even though the comparison of different catalysts is always a hard task because of the heterogeneity of reaction conditions, the results highlight that **TSP-Mg-imi** possesses excellent catalytic activity if compared with several previously reported heterogeneous bifunctional metalloporphyrin-based catalysts (see Table S2). Moreover, considering

Table 2

Cyclic carbonates synthesis catalyzed by **TSP-Mg-imi**.[a]

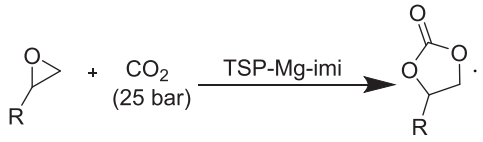

Entry	Substrate	t(h)	T (° C)	Conversion (%)[b]	TON_{Mg}[c]	TOF_{Mg} (h^{-1})[c]	Productivity[d]
1[e,f]	 237 mmol	24	150	75	2300	95	100
2	 210 mmol	3	125	56	6200	2100	300
3	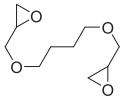 131 mmol	20	125	95	13,100	660	1200
4	 355 mmol	3	100	32	6000	2000	200
5[g]	 231 mmol	24	150	70	8500	360	300

[a] Reaction conditions: CO_2 (25 bar), catalyst 60 mg (0.019 mmol Mg), 500 rpm.
[b] Determined by ^{1}H NMR.
[c] TON_{Mg} and TOF_{Mg} values calculated based on the Mg content obtained from ICP analysis.
[d] productivity (P, calculated as grams of cyclic carbonates obtained *per* grams of catalyst).
[e] Catalyst 240 mg (0.079 μmol Mg).
[f] Selectivity toward cyclic carbonates 96% (*cis/trans* ratio 94:6).
[g] Selectivity toward polycarbonates 90%.

that the reaction conditions can be easily adapted to obtain full conversion with a selectivity higher than 95 %, and that the process takes place under solvent free conditions, in the presence of a reusable heterogeneous catalyst, the overall process is highly sustainable (with an E-factor close to zero).

The reaction conditions used here to convert CO_2 required a temperature range of 30–150 °C, using a pressure of 25 bar for each run. These conditions may appear as not mild, but we must consider that our reactor operates with large amounts of epoxide (usually more than 200 mmol). The use of only one equivalent of CO_2 at atmospheric pressure would require the filling of a volume of almost 5 L at room temperature, hence the high pressure used instead. One of the goals of the process intensification [81] is the reduction in the size and/or volume of all the process plant components. High CO_2 pressures make it possible to significantly reduce the reactor volume. For instance, the industrial production of propylene carbonate can be carried out within a reactor operating at high pressures (20 bar) at 180 °C in the presence of a homogeneous catalyst [82].

4. Conclusions

In the present work, magnesium tetrastyrylporphyrin (**TSP-Mg**) and bis(vinyl)imidazolium salt **5** have been polymerized in the presence (**7a** and **7b**) or in the absence (**TSP-Mg-imi**) of multi-walled carbon nanotubes. The corresponding highly cross-linked materials have been characterized by means of several spectroscopic and analytical techniques such as TGA, TEM, SEM-EDX, ICP-OES, XPS, solid state NMR, porosimetry. **TSP-Mg-imi** possesses a high specific surface area for this kind of cross-linked materials resulting in good performances as heterogeneous catalyst in the cycloaddition reaction of CO_2 to epoxides to afford the corresponding cyclic carbonates under solvent-free conditions. In the same conditions, the nanotube-based analogue **7a** displayed poor performances. An improvement in the catalytic activity has been achieved with the hybrid **7b** with a 1:8 Mg/Br^- ratio in the final material. However, the unsupported material **TSP-Mg-imi** has been elected as the catalyst of choice due to its easier preparation and cheaper cost, resulting in highly active in the formation of cyclic carbonates and recyclable for at least four cycles. Additional tests proved a superior activity for **TSP-Mg-imi** under heterogeneous catalysis conditions compared to the corresponding [**Bis-imi** + T**SP-Mg**] homogeneous system. The enhanced activity of the bifunctional catalyst can be ascribed to its high surface area, which permits full access to the catalytic sites, combined with the proximity between the metal centers and the bromide ions due to the covalent link between the porphyrin core and the bis(vinyl)imidazolium salt, enabling a strong cooperation that results in a synergistic effect during the catalytic cycle, as also highlighted by the computational results. The metalloporphyrin moiety acts both as a sort of "covalent swelling agent" giving rise to a higher surface area and as a Lewis acid co-catalytic species.

Declaration of Competing Interest

The authors declare the following financial interests/personal relationships which may be considered as potential competing interests: [Francesco Giacalone reports financial support was provided by Government of Italy Ministry of Education University and Research. Roberto Lazzaroni reports financial support was provided by Walloon Region. Carmela Aprile and Roberto Lazzaroni reports financial support was provided by European Regional Development Fund. Roberto Lazzaroni reports financial support was provided by Fonds National de la Recherche Scientifique. Carmela Aprile reports financial support was provided by Fonds National de la Recherche Scientifique].

Data availability

Data will be made available on request.

Acknowledgements

The authors gratefully acknowledge the University of Palermo and the Italian Ministry of Education, University and Research (MIUR) for financial support through PRIN 2017 [project no. 2017W8KNZW]. The Namur-Mons collaboration is supported by the European Regional Development Fund (FEDER) and the Walloon Region (Low Carbon Footprint Materials – BIORG-EL project). Research in Mons is also supported by the Fonds National de la Recherche Scientifique (F.R.S.-FNRS) [grant 2.5020.11] 'Consortium des Équipements de Calcul Intensif (CÉCI)' and the Walloon Region [grant 1117545] (Tier-1 supercomputer of the Fédération Wallonie-Bruxelles). Research in Namur is also supported by FNRS via the research project [grant G 4/1/6-GEQ/CDB and PDR T.0004.21]. This research used resources of PC2 (Plateforme Technologique Physico-Chemical Characterization), SIAM (Synthesis, Irradiation & Analysis of Materials) and MORPH-IM (Morphology & Imaging) technology platforms located at the University of Namur.

Appendix A. Supplementary data

Supplementary data to this article can be found online at https://doi.org/10.1016/j.jcat.2023.115143.

References

[1] T. Sakakura, J.-C. Choi, H. Yasuda, Transformation of carbon dioxide, Chem. Rev. 107 (2007) 2365–2387, https://doi.org/10.1021/cr068357u.
[2] X. Wu, C. Chen, Z. Guo, M. North, A.C. Whitwood, Metal- and halide-free catalyst for the synthesis of cyclic carbonates from epoxides and carbon dioxide, ACS Catal. 9 (2019) 1895–1906, https://doi.org/10.1021/acscatal.8b04387.
[3] A. Dibenedetto, A. Angelini, P. Stufano, Use of carbon dioxide as feedstock for chemicals and fuels: Homogeneous and heterogeneous catalysis, J. Chem. Technol. Biotechnol. 89 (2014) 334–353, https://doi.org/10.1002/jctb.4229.
[4] M. Aresta, A. Dibenedetto, A. Angelini, Catalysis for the valorization of exhaust carbon: From CO_2 to chemicals, materials, and fuels. technological use of CO_2, Chem. Rev. 114 (2014) 1709–1742, https://doi.org/10.1021/cr4002758.
[5] X.-B. Lu, D.J. Darensbourg, Cobalt catalysts for the coupling of CO2 and epoxides to provide polycarbonates and cyclic carbonates, Chem. Soc. Rev. 41 (2012) 1462–1484, https://doi.org/10.1039/C1CS15142H.
[6] Z. Qin, C.M. Thomas, S. Lee, G.W. Coates, Cobalt-based complexes for the copolymerization of propylene oxide and CO2: Active and selective catalysts for polycarbonate synthesis, Angew. Chem. Int. Ed. 42 (2003) 5484–5487, https://doi.org/10.1002/anie.200352605.
[7] K. Huang, J.-Y. Zhang, F. Liu, S. Dai, Synthesis of porous polymeric catalysts for the conversion of carbon dioxide, ACS Catal. 8 (2018) 9079–9102, https://doi.org/10.1021/acscatal.8b02151.
[8] C. Maeda, Y. Miyazaki, T. Ema, Recent progress in catalytic conversions of carbon dioxide, Catal Sci. Technol. 4 (2014) 1482–1497, https://doi.org/10.1039/C3CY00993A.
[9] E.A. Quadrelli, G. Centi, J.-L. Duplan, S. Perathoner, Carbon dioxide recycling: Emerging large-scale technologies with industrial potential, ChemSusChem 4 (2011) 1194–1215, https://doi.org/10.1002/cssc.201100473.
[10] M. North, R. Pasquale, C. Young, Synthesis of cyclic carbonates from epoxides and CO2, Green Chem. 12 (2010) 1514–1539, https://doi.org/10.1039/C0GC00065E.
[11] R.R. Shaikh, S. Pornpraprom, V. D'Elia, Catalytic strategies for the cycloaddition of pure, diluted, and waste CO2 to epoxides under ambient conditions, ACS Catal. 8 (2018) 419–450, https://doi.org/10.1021/acscatal.7b03580.
[12] T. Sakakura, K. Kohno, The synthesis of organic carbonates from carbon dioxide, Chem. Commun. (2009) 1312–1330, https://doi.org/10.1039/B819997C.
[13] B. Schäffner, F. Schäffner, S.P. Verevkin, A. Börner, Organic carbonates as solvents in synthesis and catalysis, Chem. Rev. 110 (2010) 4554–4581, https://doi.org/10.1021/cr900393d.
[14] R.B. Mujmule, W.-J. Chung, H. Kim, Chemical fixation of carbon dioxide catalyzed via hydroxyl and carboxyl-rich glucose carbonaceous material as a heterogeneous catalyst, Chem. Eng. J. 395 (2020) 125164, https://doi.org/10.1016/j.cej.2020.125164.
[15] J.A. Castro-Osma, K.J. Lamb, M. North, Cr(salophen) complex catalyzed cyclic carbonate synthesis at ambient temperature and pressure, ACS Catal. 6 (2016) 5012–5025, https://doi.org/10.1021/acscatal.6b01386.
[16] F. de la Cruz-Martínez, J.A. Castro-Osma, A. Lara-Sánchez, Carbon dioxide fixation into cyclic carbonates at room temperature catalyzed by heteroscorpionate aluminum complexes, Green Chem. Eng. 3 (2022) 280–287, https://doi.org/10.1016/j.gce.2022.02.003.
[17] F. de la Cruz-Martínez, J. Martínez, M.A. Gaona, J. Fernández-Baeza, L.F. Sánchez-Barba, A.M. Rodríguez, J.A. Castro-Osma, A. Otero, A. Lara-Sánchez, Bifunctional aluminum catalysts for the chemical fixation of carbon dioxide into cyclic carbonates, ACS Sustain. Chem. Eng. 6 (2018) 5322–5332, https://doi.org/10.1021/acssuschemeng.8b00102.

[18] M. Faizan, N. Srivastav, R. Pawar, Azaboratrane as an exceptionally potential organocatalyst for the activation of CO_2 and coupling with epoxide, Mol. Catal. 521 (2022) 112201, https://doi.org/10.1016/j.mcat.2022.112201.

[19] la Cruz-Martínez F.d. M.M.d. Sarasa Buchaca J. Fernández-Baeza L.F. Sánchez-Barba A.M. Rodríguez C. Alonso-Moreno J.A. Castro-Osma, and A. Lara-Sánchez, Heteroscorpionate Rare-Earth Catalysts for the Low-Pressure Coupling Reaction of CO_2 and Cyclohexene Oxide, Organometallics 40 (2021) 1503-1514, doi: 10.1021/acs.organomet.1c00164.

[20] Y. Lei, H.Q.N. Gunaratne, L. Jin, Design and synthesis of pyridinamide functionalized ionic liquids for efficient conversion of carbon dioxide into cyclic carbonates, J. CO2 Util. 58 (2022) 101930, https://doi.org/10.1016/j.jcou.2022.101930.

[21] M.-R. Li, M.-C. Zhang, T.-J. Yue, X.-B. Lu, W.-M. Ren, Highly efficient conversion of CO_2 to cyclic carbonates with a binary catalyst system in a microreactor: intensification of "electrophile–nucleophile" synergistic effect, RSC Adv. 8 (2018) 39182–39186, https://doi.org/10.1039/C8RA07236A.

[22] Y. Liu, Z. Cao, Z. Zhou, A. Zhou, Imidazolium-based deep eutectic solvents as multifunctional catalysts for multisite synergistic activation of epoxides and ambient synthesis of cyclic carbonates, J. CO2 Util. 53 (2021) 101717, https://doi.org/10.1016/j.jcou.2021.101717.

[23] L. Qu, I. del Rosal, Q. Li, Y. Wang, D. Yuan, Y. Yao, L. Maron, Efficient CO2 transformation under ambient condition by heterobimetallic rare earth complexes: Experimental and computational evidences of a synergistic effect, J. CO2 Util. 33 (2019) 413–418, https://doi.org/10.1016/j.jcou.2019.07.008.

[24] V.B. Saptal, B.M. Bhanage, Bifunctional ionic liquids derived from biorenewable sources as sustainable catalysts for fixation of carbon dioxide, ChemSusChem 10 (2017) 1145–1151, https://doi.org/10.1002/cssc.201601228.

[25] C.J. Whiteoak, E. Martin, M.M. Belmonte, J. Benet-Buchholz, A.W. Kleij, An efficient iron catalyst for the synthesis of five- and six-membered organic carbonates under mild conditions, Adv. Synth. Catal. 354 (2012) 469–476, https://doi.org/10.1002/adsc.201100752.

[26] R. Luo, M. Chen, X. Liu, W. Xu, J. Li, B. Liu, Y. Fang, Recent advances in CO2 capture and simultaneous conversion into cyclic carbonates over porous organic polymers having accessible metal sites, J. Mater. Chem. A 8 (2020) 18408–18424, https://doi.org/10.1039/D0TA06142E.

[27] T.K. Pal, D. De, P.K. Bharadwaj, Metal-organic frameworks as heterogeneous catalysts for the chemical conversion of carbon dioxide, Fuel 320 (2022) 123904, https://doi.org/10.1016/j.fuel.2022.123904.

[28] L.A. Siddig, R.H. Alzard, H.L. Nguyen, C.R. Göb, M.A. Alnaqbi, A. Alzamly, Hexagonal layer manganese metal-organic framework for photocatalytic CO2 cycloaddition reaction, ACS Omega 7 (2022) 9958–9963, https://doi.org/10.1021/acsomega.2c00663.

[29] J. Tapiador, P. Leo, A. Rodríguez-Diéguez, D. Choquesillo-Lazarte, G. Calleja, G. Orcajo, A novel Zn-based-MOF for efficient CO_2 adsorption and conversion under mild conditions, Catal. Today 390–391 (2022) 230–236, https://doi.org/10.1016/j.cattod.2021.11.025.

[30] W. Wang, C. Li, J. Jin, L. Yan, Y. Ding, Mg–porphyrin complex doped divinylbenzene based porous organic polymers (POPs) as highly efficient heterogeneous catalysts for the conversion of CO2 to cyclic carbonates, Dalton Trans. 47 (2018) 13135–13141, https://doi.org/10.1039/C8DT02913J.

[31] R. Luo, W. Zhang, Z. Yang, X. Zhou, H. Ji, Synthesis of cyclic carbonates from epoxides over bifunctional salen aluminum oligomers as a CO2-philic catalyst: Catalytic and kinetic investigation, J. CO2 Util. 19 (2017) 257–265, https://doi.org/10.1016/j.jcou.2017.04.002.

[32] L. Liu, S. Jayakumar, J. Chen, L. Tao, H. Li, Q. Yang, C. Li, Synthesis of bifunctional porphyrin polymers for catalytic conversion of dilute CO2 to cyclic carbonates, ACS Appl. Mater. Interfaces 13 (2021) 29522–29531, https://doi.org/10.1021/acsami.1c04624.

[33] Z. Su, L. Ma, J. Wei, X. Bai, N. Wang, J. Li, A zinc porphyrin polymer as efficient bifunctional catalyst for conversion of CO2 to cyclic carbonates, Appl. Organomet. Chem. 36 (2022) e6632, https://doi.org/10.1002/aoc.6632.

[34] W. Wang, Y. Wang, C. Li, L. Yan, M. Jiang, Y. Ding, State-of-the-art multifunctional heterogeneous POP catalyst for cooperative transformation of CO2 to cyclic carbonates, ACS Sustain. Chem. Eng. 5 (2017) 4523–4528, https://doi.org/10.1021/acssuschemeng.7b00947.

[35] X. Bai, Z. Su, J. Wei, L. Ma, S. Duan, N. Wang, X. Zhang, J. Li, Zinc(II)porphyrin-based porous ionic polymers (PIPs) as multifunctional heterogeneous catalysts for the conversion of CO2 to cyclic carbonates, Ind. Eng. Chem. Res. 61 (2022) 5093–5102, https://doi.org/10.1021/acs.iecr.2c00161.

[36] Q.-J. Wu, M.-J. Mao, J.-X. Chen, Y.-B. Huang, R. Cao, Integration of metalloporphyrin into cationic covalent triazine frameworks for the synergistically enhanced chemical fixation of CO2, Catal, Sci. Technol. 10 (2020) 8026–8033, https://doi.org/10.1039/D0CY01636E.

[37] H. He, Q.-Q. Zhu, W.-W. Zhang, H.-W. Zhang, J. Chen, C.-P. Li, M. Du, Metal and Co-Catalyst Free CO2 conversion with a bifunctional covalent organic framework (COF), ChemCatChem 12 (2020) 5192–5199, https://doi.org/10.1002/cctc.202000949.

[38] Y. Chen, R. Luo, Q. Xu, J. Jiang, X. Zhou, H. Ji, Charged metalloporphyrin polymers for cooperative synthesis of cyclic carbonates from CO2 under ambient conditions, ChemSusChem 10 (2017) 2534–2541, https://doi.org/10.1002/cssc.201700536.

[39] R. Luo, Y. Chen, Q. He, X. Lin, Q. Xu, X. He, W. Zhang, X. Zhou, H. Ji, Metallosalen-based ionic porous polymers as bifunctional catalysts for the conversion of CO2 into valuable chemicals, ChemSusChem 10 (2017) 1526–1533, https://doi.org/10.1002/cssc.201601846.

[40] H. Li, C. Li, J. Chen, L. Liu, Q. Yang, Synthesis of a pyridine–zinc-based porous organic polymer for the co-catalyst-free cycloaddition of epoxides, Chem. Asian J. 12 (2017) 1095–1103, https://doi.org/10.1002/asia.201700258.

[41] D. Ma, B. Li, K. Liu, X. Zhang, W. Zou, Y. Yang, G. Li, Z. Shi, S. Feng, Bifunctional MOF heterogeneous catalysts based on the synergy of dual functional sites for efficient conversion of CO2 under mild and co-catalyst free conditions, J. Mater. Chem. A 3 (2015) 23136–23142, https://doi.org/10.1039/C5TA07026K.

[42] J. Liu, G. Zhao, O. Cheung, L. Jia, Z. Sun, S. Zhang, Highly porous metalloporphyrin covalent ionic frameworks with well-defined cooperative functional groups as excellent catalysts for CO_2 cycloaddition, Chem. Eur. J. 25 (2019) 9052–9059, https://doi.org/10.1002/chem.201900992.

[43] R. Luo, M. Chen, F. Zhou, J. Zhan, Q. Deng, Y. Yu, Y. Zhang, W. Xu, Y. Fang, Synthesis of metalloporphyrin-based porous organic polymers and their functionalization for conversion of CO_2 into cyclic carbonates: Recent advances, opportunities and challenges, J. Mater. Chem. A 9 (2021) 25731–25749, https://doi.org/10.1039/D1TA08146B.

[44] W.-Y. Gao, M. Chrzanowski, S. Ma, Metal–metalloporphyrin frameworks: a resurging class of functional materials, Chem. Soc. Rev. 43 (2014) 5841–5866, https://doi.org/10.1039/C4CS00001C.

[45] K. Tashiro, T. Aida, Metalloporphyrin hosts for supramolecular chemistry of fullerenes, Chem. Soc. Rev. 36 (2007) 189–197, https://doi.org/10.1039/B614883M.

[46] Z. Dai, Y. Tang, F. Zhang, Y. Xiong, S. Wang, Q. Sun, L. Wang, X. Meng, L. Zhao, F.-S. Xiao, Combination of binary active sites into heterogeneous porous polymer catalysts for efficient transformation of CO_2 under mild conditions, Chin. J. Catal. 42 (2021) 618–626, https://doi.org/10.1016/S1872-2067(20)63679-8.

[47] T. Ema, Y. Miyazaki, S. Koyama, Y. Yano, T. Sakai, A bifunctional catalyst for carbon dioxide fixation: cooperative double activation of epoxides for the synthesis of cyclic carbonates, Chem. Commun. 48 (2012) 4489–4491, https://doi.org/10.1039/C2CC30591G.

[48] T. Ema, Y. Miyazaki, J. Shimonishi, C. Maeda, J.-Y. Hasegawa, Bifunctional porphyrin catalysts for the synthesis of cyclic carbonates from epoxides and CO_2: Structural optimization and mechanistic study, J. Am. Chem. Soc. 136 (2014) 15270–15279, https://doi.org/10.1021/ja507665a.

[49] C. Maeda, J. Shimonishi, R. Miyazaki, J.-Y. Hasegawa, T. Ema, Frontispiece: Highly active and robust metalloporphyrin catalysts for the synthesis of cyclic carbonates from a broad range of epoxides and carbon dioxide, Chem. Eur. J. 22 (2016) 6556–6563, https://doi.org/10.1002/chem.201681962.

[50] V. Campisciano, L. Valentino, A. Morena, A. Santiago-Portillo, N. Saladino, M. Gruttadauria, C. Aprile, F. Giacalone, Carbon nanotube supported aluminum porphyrin-imidazolium bromide crosslinked copolymer: A synergistic bifunctional catalyst for CO2 conversion, J. CO2 Util. 57 (2022) 101884, https://doi.org/10.1016/j.jcou.2022.101884.

[51] A. Morena, V. Campisciano, A. Santiago-Portillo, M. Gruttadauria, F. Giacalone, C. Aprile, POSS-Al-porphyrin-imidazolium cross-linked network as catalytic bifunctional platform for the conversion of CO_2 with epoxides, Fuel 336 (2022) 126819, doi:10.1016/j.fuel.2022.126819.

[52] M. Buaki-Sogó, A. Vivian, L.A. Bivona, H. García, M. Gruttadauria, C. Aprile, Imidazolium functionalized carbon nanotubes for the synthesis of cyclic carbonates: reducing the gap between homogeneous and heterogeneous catalysis, Catal. Sci. Technol. 6 (2016) 8418–8427, https://doi.org/10.1039/C6CY01068G.

[53] P. Agrigento, S.M. Al-Amsyar, B. Sorée, M. Taherimehr, M. Gruttadauria, C. Aprile, P.P. Pescarmona, Synthesis and high-throughput testing of multilayered supported ionic liquid catalysts for the conversion of CO2 and epoxides into cyclic carbonates, Catal. Sci. Technol. 4 (2014) 1598–1607, https://doi.org/10.1039/C3CY01000G.

[54] C. Aprile, F. Giacalone, P. Agrigento, L.F. Liotta, J.A. Martens, P.P. Pescarmona, M. Gruttadauria, Multilayered supported ionic liquids as catalysts for chemical fixation of carbon dioxide: A high-throughput study in supercritical conditions, ChemSusChem 4 (2011) 1830–1837, https://doi.org/10.1002/cssc.201100446.

[55] C. Calabrese, L.F. Liotta, E. Carbonell, F. Giacalone, M. Gruttadauria, C. Aprile, Imidazolium-functionalized carbon nanohorns for the conversion of carbon dioxide: Unprecedented increase of catalytic activity after recycling, ChemSusChem 10 (2017) 1202–1209, https://doi.org/10.1002/cssc.201601427.

[56] C. Calabrese, L.F. Liotta, F. Giacalone, M. Gruttadauria, C. Aprile, Supported polyhedral oligomeric silsesquioxane-Based (POSS) Materials as Highly Active Organocatalysts for the Conversion of CO2, ChemCatChem 11 (2019) 560–567, https://doi.org/10.1002/cctc.201801351.

[57] L.A. Bivona, O. Fichera, L. Fusaro, F. Giacalone, M. Buaki-Sogo, M. Gruttadauria, C. Aprile, A polyhedral oligomeric silsesquioxane-based catalyst for the efficient synthesis of cyclic carbonates, Catal Sci. Technol. 5 (2015) 5000–5007, https://doi.org/10.1039/C5CY00830A.

[58] C. Cadena, J.L. Anthony, J.K. Shah, T.I. Morrow, J.F. Brennecke, E.J. Maginn, Why Is CO2 So soluble in imidazolium-based ionic liquids? J. Am. Chem. Soc. 126 (2004) 5300–5308, https://doi.org/10.1021/ja039615x.

[59] J.M. Zhu, K.G. He, H. Zhang, F. Xin, Effect of swelling on carbon dioxide adsorption by poly(Ionic Liquid)s, Adsorp. Sci. Technol. 30 (2012) 35–41, https://doi.org/10.1260/0263-6174.30.1.35.

[60] S. Zulfiqar, M.I. Sarwar, D. Mecerreyes, Polymeric ionic liquids for CO2 capture and separation: potential, progress and challenges, Polym. Chem. 6 (2015) 6435–6451, https://doi.org/10.1039/C5PY00842E.

[61] J. Tang, H. Tang, W. Sun, H. Plancher, M. Radosz, Y. Shen, Poly(ionic liquid)s: a new material with enhanced and fast CO2 absorption, Chem. Commun. (2005) 3325–3327, https://doi.org/10.1039/B501940K.

[62] F. Giacalone, M. Gruttadauria, Covalently supported ionic liquid phases: An advanced class of recyclable catalytic systems, ChemCatChem 8 (2016) 664–684, https://doi.org/10.1002/cctc.201501086.

[63] V. Campisciano, F. Giacalone, M. Gruttadauria, Supported ionic liquids: A versatile and useful class of materials, Chem. Rec. 17 (2017) 918–938, https://doi.org/10.1002/tcr.201700005.
[64] V. Campisciano, M. Gruttadauria, F. Giacalone, Modified nanocarbons for catalysis, ChemCatChem 11 (2019) 90–133, https://doi.org/10.1002/cctc.201801414.
[65] V. Campisciano, M. Gruttadauria, F. Giacalone, Modified Nanocarbons as Catalysts in Organic Processes In "Catalyst Immobilization: Methods and Applications"; Benaglia, M., Puglisi, A., Eds.; Wiley-VCH: Weinheim, Germany, 2019; pp. 77–113.
[66] V. Campisciano, R. Burger, C. Calabrese, L.F. Liotta, P. Lo Meo, M. Gruttadauria, F. Giacalone, Straightforward preparation of highly loaded MWCNT–polyamine hybrids and their application in catalysis, Nanoscale Adv. 2 (2020) 4199–4211, https://doi.org/10.1039/D0NA00291G.
[67] V. Campisciano, C. Calabrese, L.F. Liotta, V. La Parola, A. Spinella, C. Aprile, M. Gruttadauria, F. Giacalone, Templating effect of carbon nanoforms on highly cross-linked imidazolium network: Catalytic activity of the resulting hybrids with Pd nanoparticles, Appl. Organomet. Chem. 33 (2019) e4848.
[68] S. Grimme, S. Ehrlich, L. Goerigk, Effect of the damping function in dispersion corrected density functional theory, J. Comput. Chem. 32 (2011) 1456–1465, https://doi.org/10.1002/jcc.21759.
[69] S. Simon, M. Duran, J.J. Dannenberg, How does basis set superposition error change the potential surfaces for hydrogen-bonded dimers? J. Chem. Phys. 105 (1996) 11024–11031, https://doi.org/10.1063/1.472902.
[70] E.I. García-López, V. Campisciano, F. Giacalone, L.F. Liotta, G. Marcì, Supported Poly(Ionic Liquid)-heteropolyacid based materials for heterogeneous catalytic fructose dehydration in aqueous medium, Molecules 27 (2022) 4722, https://doi.org/10.3390/molecules27154722.
[71] R. Buscemi, F. Giacalone, S. Orecchio, M. Gruttadauria, Cross-linked imidazolium salts as scavengers for palladium, ChemPlusChem 79 (2014) 421–426, https://doi.org/10.1002/cplu.201300361.
[72] A. Morena, V. Campisciano, A. Comès, L.F. Liotta, M. Gruttadauria, C. Aprile, F. Giacalone, A Study on the stability of carbon nanoforms-polyimidazolium network hybrids in the conversion of CO2 into Cyclic Carbonates: Increase in catalytic activity after reuse, Nanomaterials 11 (2021) 2243, https://doi.org/10.3390/nano11092243.
[73] M. Thommes, K. Kaneko, A.V. Neimark, J.P. Olivier, F. Rodriguez-Reinoso, J. Rouquerol, K.S.W. Sing, Physisorption of gases, with special reference to the evaluation of surface area and pore size distribution (IUPAC Technical Report), Pure Appl. Chem. 87 (2015) 1051–1069, https://doi.org/10.1515/pac-2014-1117.
[74] C. Pavia, E. Ballerini, L.A. Bivona, F. Giacalone, C. Aprile, L. Vaccaro, M. Gruttadauria, Palladium Supported on cross-linked imidazolium network on silica as highly sustainable catalysts for the suzuki reaction under flow conditions, Adv. Synth. Catal. 355 (2013) 2007–2018, https://doi.org/10.1002/adsc.201300215.
[75] H. Song, Y. Wang, M. Xiao, L. Liu, Y. Liu, X. Liu, H. Gai, Design of novel poly(ionic liquids) for the conversion of CO2 to Cyclic Carbonates under mild conditions without solvent, ACS Sustain. Chem. Eng. 7 (2019) 9489–9497, https://doi.org/10.1021/acssuschemeng.9b00865.
[76] J. Yuan, D. Mecerreyes, M. Antonietti, Poly(ionic liquid)s: An update, Prog. Polym. Sci. 38 (2013) 1009–1036, https://doi.org/10.1016/j.progpolymsci.2013.04.002.
[77] S. Muralidharan, R. Hayes, Intense satellites in the N 1s X-ray photoelectron spectra of certain metalloporphyrins, J. Am. Chem. Soc. 102 (1980) 5106–5107, doi: 10.1021/ja00535a052..
[78] D.H. Karweik, N. Winograd, Nitrogen charge distributions in free-base porphyrins, metalloporphyrins, and their reduced analogs observed by x-ray photoelectron spectroscopy, Inorg. Chem. 15 (1976) 2336–2342, https://doi.org/10.1021/ic50164a003.
[79] J. Zhang, P. Zhang, Z. Zhang, X. Wei, Spectroscopic and kinetic studies of photochemical reaction of magnesium tetraphenylporphyrin with oxygen, Chem. A Eur. J. 113 (2009) 5367–5374, https://doi.org/10.1021/jp811209k.
[80] J. Huang, C. Jehanno, J.C. Worch, F. Ruipérez, H. Sardon, A.P. Dove, O. Coulembier, Selective organocatalytic preparation of trimethylene carbonate from oxetane and carbon dioxide, ACS Catal. 10 (2020) 5399–5404, https://doi.org/10.1021/acscatal.0c00689.
[81] D. Reay, C. Ramshaw, A. Harvey, Chapter 1 - A Brief History of Process Intensification, in: D. Reay, C. Ramshaw, A. Harvey (Eds.), Process Intensification (second Edition), Butterworth-Heinemann, Oxford, 2013, pp. 1–25.
[82] J.P. Lange, US Patent 7728164B2 (2010) to Shell Oil Company.